DR-136

ERDA/JPL/954344–76/1

WEB-DENDRITIC RIBBON GROWTH

USC solar report No. Q-2

Quarterly report, 1 January 1976–31 March 1976

R. B. Hilborn, Jr
J. W. Faust, Jr.

March 17, 1976

Work performed under contract No. 954344

College of Engineering
University of South Carolina
Columbia, South Carolina

ENERGY RESEARCH AND DEVELOPMENT ADMINISTRATION
Division of Solar Energy

DISCLAIMER

Available from the National Technical Information Service, U. S. Department of Commerce, Springfield, Virginia 22161

Price: Paper Copy $4.00 (domestic)
$6.50 (foreign)
Microfiche $2.25 (domestic)
$3.75 (foreign)

Printed in the United States of America
USERDA Technical Information Center, Oak Ridge, Tennessee

ERDA/JPL/954344-76/1
Distribution Category UC-63

Web-Dendritic Ribbon Growth

USC Solar Report No. Q-2

Quarterly Report for Period 1-1-76 to 3-31-76

Authors: R. B. Hilborn, Jr. and J. W. Faust, Jr.

Date of Publication: 3-17-76

JPL Contract No. 954344

Contractor: University of South Carolina
College of Engineering
Columbia, S.C. 29208

This work was performed for the Jet Propulsion Laboratory, California Institute of Technology, under NASA Contract NAS7-100 for the U.S. Energy Research and Development Administration, Division of Solar Energy.

The JPL Low-cost Silicon Solar Array Project is funded by ERDA and forms part of the ERDA Photovoltaic Conversion Program to initiate a major effort toward the development of low-cost solar arrays.

TABLE OF CONTENTS

SUBJECT	PAGE
Technical Content Statement	1
Abstract	1
Man-hours and Cost Totals	1
Summary of Results	1-2
Review by Task Element	3
Table 1	16
Table 2	17
Figure 1	18
Figure 2	19
Figure 3	19
Figure 4	20
Figure 5	21
Figure 6	22
Figure 7	23
Figure 8	24
Figure 9	25
Figure 10	26
Figure 11	27
Program Plan	Attachment

Technical Content Statement

This report contains information prepared by the University of South Carolina under JPL subcontract. Its content is not necessarily endorsed by the Jet Propulsion Laboratory, California Institute of Technology, National Aeronautics and Space Administration, or the U.S. Energy Research and Development Administration, Division of Solar Energy.

Abstract

This is a report of the second quarter's work on the web-dendritic ribbon growth at the University of South Carolina. A brief description of the work initiated and carried out during this period to meet the program goals is given along with a copy of the Program Plan covering the entire period of the contract.

Man-hours and Cost Totals

Previous		Current Quarter		Cumulative	
Man-hours	Cost	Man-hours	Cost	Man-hours	Cost
1977	$25,719	3160	$40,157	5137	$65,876

Summary of Results

The purpose of this investigation is to develop web-dendritic process methods that will: (1) minimize the cost of processing silicon into ribbons of solar cell quality with a terrestrial energy conversion efficiency greater than 10%, and (2) be suitable for large quantity production.

The goals for producing silicon ribbon by the web-dendritic process developed under this contract are:

Width	5.0 cms
Linear Growth Rate	5 cms/minute
Thickness	4 mils $\pm$ 1 mil
Dislocation Density	$< 10^4$ cm^{-2}
Crystal Structure	Single Crystal

The work is largely experimental in nature, utilizing the results of thermal modeling analyses and empirically determined data from ribbon growth runs to determine the feasibility of the process methods.

The report for this second quarter describes the work of the program during this period and presents the plan for the program for the full length of the contract.

Work is described on:

(1) the procedures used to calibrate and operate the web-dendritic growth furnace;

(2) use of the furnace to grow web-dendritic ribbon;

(3) considerations applied for the thermal analysis and modeling of the web-dendritic growth system;

(4) procedures, facilities and initial results for the structural and electrical characterization of web material.

The major result of this report period is the successful growth of web-dendritic ribbon.

We are on schedule in regard to our time-phased program plan.

In view of the apparent progress being made towards the attainment of the program goals, no recommended changes in the initial program plan are offered at this time.

Review by Task Element

T.E. 1.2.1: Pull nominal web based on 1965 experience; establish measurements baseline.

In the first quarterly report (Q-1), the thermal probing of the melt and the steps to shape the thermal geometry that finally lead to the successful pulling of several feet of dendrites were reported. It was also reported that "within the next few days web pulling will begin." It was begun; the first webs grown were, understandably, "third dendrite" type of web. (This is the term given to describe webs with one - true third dendrite web - or more dendrites in the web region between the edge dendrites.) This along with other observations, namely (a) the center of thermal symmetry varied from day to day, (b) occasionally ice formed in the melt after a foot or so of web had been pulled, and (c) the button and resulting web growth was not always symmetrical, showed that more work had to be done on shaping the thermal gradients not only on the surface but also in the depth of the melt. The work that was done during this report period that resulted in the growth of good webs is briefly summarized below, although not necessarily in the order in which it was done.

1. Positioning of the susceptor in relation to the r.f. coil. Some work of this nature had been done in the last report period. This time it was done more systematically. Temperature measurements were made on the top of the heat shield and directly below on the bottom of the susceptor for eight positions of the susceptor in the work coil. This data is given in Table 1 and graphed in Figure 1. From this graph we can choose our best position on the scale attached to our vertical adjustment column.

2. The shape of the susceptor was changed to give more heat input at the lower part of the susceptor.

3. Changed the drive wheel to the pulling reel to give us added range at the lower end of the scale.

4. Went to a thicker heat shield to overcome a problem of bowing of the shields.

5. Changed shape of slot in heat shield. The first slot used was wide; the second narrow. Then to decrease further the supercooling in the center, holes were drilled at the ends of the slot giving a shape of a "dog bone." A further shaping was done giving a shape sketched in Figure 2.

6. We have occasionally had a "bad" seed; i.e., a button did not form or the button had an unfavorable shape. Figure 3 shows a button with a single twin (i.e., the other two twins were "lost" in seeding as a twin lamella). We are cataloging all of our webs and dendrites to find other twin spacings. We feel that the present twin spacing is too narrow. The optimum twin spacing in silicon was never determined as it was in the case of germanium.

7. Several additions have been made in the start-up routine to insure a uniform "starting point." These involve leveling of the melt by adjustment of the Serva-Levl legs, checking symmetry of work coil, and checking thermal symmetry with a seed.

The effect of this shaping of the isotherms thus far has been reflected in longer pulls, more pulls with "good" two dendrite web, and more control over the seeding. Much of the data collected and reported in this Task Element actually falls under other Task Elements - especially 1.2.2 and 1.2.3.

During the next three-month period work will continue in the following ways: (a) put x-y motion on the work coil; (b) use other twin spacings; (c) install additonal radiation shielding at the top; (d) install radiation shield under susceptor; (e) install heat insulation between pedestal and susceptor; and (f) physically shape the susceptor.

T.E. 1.2.2: Vary pull rate; measure effects, etc.

As mentioned above, studies of this type have been carried out and reflected in Task Element 1.2.1. Our initial range of pull rates covered pull rates of dendrites very well but was at the top of the range desired at present for pulling webs. Thus as mentioned in item 3 in Task Element 1.2.1, a smaller drive wheel was installed. With both drive wheels, the pull rate of dendrites has been varied up to "pull out." The decrease in dendrite width and thickness has been noted. "Third dendrite" webs were pulled with the larger drive wheel, but changes in pull rate were limited because of the present thermal geometry.

The change to the smaller drive wheel gave not only an improvement in the webs but also a better control over the button formation. Webs also were taken to pull-out by increasing the pull rate. No actual data on the effect of pull rate on dendrites or webs is given because the thermal conditions have been changed from pull to pull. It is also too early to attempt to correlate this data seriously with crystallization kinetics.

T.E. 1.3: Web growth analysis.

Meniscus geometry

Analysis. Theoretical studies have been performed to determine the geometry of the meniscus at the liquid-solid interface of the growing web. The meniscus geometry will have an important bearing upon the growth characteristics of the web as well as the temperature gradients at the interface.

A number of simplifying assumptions have been made which require further study; thus the results should be considered preliminary at the present time. Perhaps the most important assumption is that the static or stationary conditions were assumed. That is, the effect of fluid motion due to web growth was neglected. Uniform melt temperature and uniform constitutent concentrations were also assumed in the melt.

The shape of the meniscus is determined for static conditions using the Euler-Laplace equation which relates the pressure difference Δp across the meniscus to its curvature and the interfacial surface tension λ. That is

$$\Delta p = \lambda\left(\frac{1}{r_1} + \frac{1}{r_2} \right), \tag{1}$$

where r_1 and r_2 are the principal radii of curvature and are defined to be positive when the center of curvature is inside the region of high pressure. In the present study only the web is considered and consequently the meniscus can be considered two-dimensional and in a plane. Therefore, one of the principal radii of curvature, r_2, is infinite and $\frac{1}{r_2} = 0$.

Figure 5 is a cross-section of the web and meniscus. The angle of contact β is the angle between the solid surface and the liquid surface. Experimental measurements by Swartz, Surek, and Chalmers[1] indicate that β is approximately 11^o. Angle θ in Figure 5 is the joining angle of the meniscus and is the angle between the meniscus at contact with the solid and the vertical axis. When the top of the meniscus is located on the flat vertical surface of the web, the contact angle β and the joining angle θ are equal. Negative values of θ are measured to the left of the vertical axis and positive values to the right. Thus, the value of θ in Figure 5 would be negative.

Batchelor[2] presents the solution to the Euler-Laplace equation for the two-dimensional plane meniscus. Both the shape of the meniscus and the height can be determined from the results. Gaule and Pastore[3] derived an approximate equation for determing the meniscus height.

Following Batchelor the meniscus height h_o is given by

$$h_o = K\, 2(1-\sin\theta) \tag{2}$$

where

$$K = \frac{\Upsilon}{\rho g} \tag{3}$$

and ρ is melt density and g is the acceleration of gravity. The meniscus height h_o is also equal to the height of the interface above the melt level as long as none of the flat vertical surface is immersed in the melt. Further, the shape of the meniscus if given by

$$\frac{y}{K} = \cosh^{-1} \frac{2K}{\zeta} - \cosh^{-1} \frac{2K}{h_o} + (4 - \frac{h_o^2}{K^2})^{\frac{1}{2}} - (4 - \frac{\zeta^2}{K^2})^{\frac{1}{2}} . \quad (4)$$

When y and z are horizontal and vertical coordinates, $z = \zeta(y)$ is the liquid-gas interface. Note that h_o and ζ are functions of θ but not directly dependent on β. Angles β and θ are related by the geometry of the solid surface at the point of meniscus-solid contact.

Results of Analysis. In Figure 6 the dimensionless term h_o/K given by Equation (2) is shown as a function of θ. The maximum h_o/K is obtained when $\theta = -90^o$ and decreases to zero when $\theta = 90^o$. The results presented in Figure 2 are independent of the fluid properties and the acceleration of gravity. The terms are included in K which was defined in Equation (3). Taking the values of silicon[1] of γ = 720 erg/cm^2 and ρ = 2.49 gm/cm^3 and the acceleration of gravity of 980 cm/sec^2, it is found that K = 0.543 cm. With the value of K and Figure 6, h can be calculated by multiplying h_o/K by the value of K. For example, Mika and Uelhoff[4] state that for stationary growth (non-increasing or decreasing web thickness), θ must be approximately equal to zero. From Figure 6 the predicted value of h for stationary growth is 0.768 cm.

Figure 7 is a scale drawing of the web and melt cross-section for $\theta = 0^o$ and with a web thickness of 0.1 mm. Because of the large surface tension of silicon, a long thin column of melt is present below the web. Menisci geometries were determined using Equation (4) and are shown for various negative values of θ in Figure 8 and positive values in Figure 9. These figures show a section of the meniscus on the right side of the web and the meniscus-solid contact is along the vertical dashed line. Dimensionless coordinates y/K and ζ/K are used so that these curves are general for all fluids. In Figure 8 it is seen that the meniscus is always necked below the liquid-solid interface and the degree of necking increases as θ decreases (more negative). For positive values shown in Figure 9, the menisci are flatter and do not have the neck that occurred with negative values of θ. Note that the height of the meniscus decreases with increasing θ.

Because the webs are very thin, the menisci on the two sides of web can contact for negative values of θ so that the crystal would separate from the melt. This occurrence was not considered previously in studies of Czochralski growth since the diameter of the crystal is usually sufficiently large to prevent separation at the neck. Calculations indicate that the minimum value of θ possible without contact is approximately -10^{o} for silicon with a web thickness of 0.1 mm. The resulting section of the web and melt is shown in Figure 10. A meniscus height of 0.830 cm was determined for this condition using Figure 6 and assuming K = 0.543.

As the liquid-solid interface is lowered, the equilibrium joining angle θ has been shown to increase. As was pointed out earlier by O'Hara and Bennett[5], the web can be caused to extend into the liquid and a region of the flat web will be immersed in the melt. It was pointed out that this may not be a desirable condition since nucleation may occur on the web surface resulting in a widening of the web. As mentioned earlier, when the top of the meniscus is located on the vertical web surface the angles α and θ are equal. Assuming β equal to 11^{o} [1] then we find from Figure 2 that h_o = 0.693 cm. A section of the web and melt for this condition is shown in Figure 11. The height of the meniscus is independent of the position of the end of the web.

Discussion of Results. Studies by Gaule and Pastore[3] and Mika and Uelhoff[4] indicate that θ must be maintained at approximately zero degrees in order to obtain a uniform crystal thickness. It is predicted that the meniscus height for the silicon web would be 0.768 cm. This is also the approximate height of the interface. The magnitude of variation from this height that might be possible and still obtain flat crystals will require a thermal model. However, the results obtained in this study place some limits on the variations. The maximum height is limited by contact of the two menisci which occur at a height of 0.830 cm. Since thickening of the web may occur when the flat vertical {111} surface of the web becomes immersed in the melt, a minimum height of 0.693 cm would be possible without immersion. Further study may determine that the temperature is sufficiently near the melting point that nucleation does not occur and, therefore, the lower limit may be less than the 0.693 cm.

Work has been started on heat balance equations for the susceptor, crucible and melt. This is necessary to evaluate, and to help guide, the changes made in the furnace itself in Task Element 1.2. To help in this respect, a list of desired information is being drawn up. A sketch of the furnace to illustrate the parameters requested to date is given in Figure 4. The parameters themselves are given in Table 2.

Bibliography

1. Swartz, J.C., T. Surek, and B. Chalmers, "The EFG Process Applied to the Growth of Silicon Ribbons", J. of Electronic Materials, Vol. 4, No. 2, 1975, pp. 255-279.

2. Batchelor, G.K., An Introduction to Fluid Dynamics, Cambridge at the University Press, 1967, pp. 63-68.

3. Gaule, G.K. and J.R. Pastore, "The Role of Surface Tension in Pulling Single Crystals of Controlled Dimensions", Metallurgy of Elemental and Compound Semiconductors, Ed. by R.O. Grubel, Interscience Publishers, N.Y., 1961, pp. 201-226.

4. Mika, A. and W. Uelhoff, "Shape and Stability of Menisci in Czochralski Growth and Comparison with Analytical Approximations", Journal of Crystal Growth, Vol. 30, 1975, pp. 9-20.

5. O'Hara, S. and A.I. Bennett, "Web Growth in Semiconductors", Journal of Applied Physics, Vol. 35, No. 3, 1964, pp. 686-693.

T.E. 2.2: Structural characterization.

Lectures on structural characterization techniques and imperfections in dendrites and web were given. Because of the question of the effect of twin spacing on button formation and growth of dendrites mentioned in Task Element 1.2.1, most of the emphasis on structural characterization was placed on measuring twin spacing. Examination of the twin spacing using optical microscopy on fractured surfaces showed the twin spacing to be very narrow. Measurements were made but the resolution of the optical microscope is about .5μ; thus for one of the lamellae the narrower spacing could only be guessed at. The SEM was then used on the fractured surfaces because of its higher resolution and great depth of field. A special holder had to be made for these samples. The method is slower than OM, but is very necessary for our present narrow spacing. Attempts have been made to replicate the fractured surfaces to get the twin spacing by REM (replica electron microscopy). Thus far we have had difficulty in floating the carbon replica off the surface when we tried to use the direct carbon replica technique. We are looking into this since it worked very well for us previously on silicon. We also had trouble building up a carbon layer for the plastic replica technique. This appears to be a problem with the evaporator in the Electron Microscope Laboratory, and we are hopeful that it will soon be solved.

T.E. 2.3: Electrical characterization; web bulk silicon.

During this report period the following list of electrical characterization facilities have been completed and tested:

1. Van der Pauw
2. Four-point probe resistivity
3. Hot probe conductivity type monitor
4. MOS Minority Carrier Lifetime

These facilities have just been put to use in the characterization of web-dendritic ribbon and will continue in this service for the balance of the contract.

T.E. 2.4: Electrical characterization; web solar cells.

During this report period considerable effort has been extended in the development of an optimum processing procedure to use on the web-dendritic ribbon for making solar cells to evaluate the material. A number of process techniques have been tried and are currently being evaluated for their reproducibility and resulting device performance. This work will be completed within one month.

The facility for determining dark and illuminated i-v characteristics of solar cell samples has been completed and is operational.

Interpretation of Results and Application to Program Goals

The results to date in the growth of web-dendritic web indicate that the growth facility is working properly. The response of the facility to changes in growth conditions indicate that it will be suitable for testing new concepts and experiments suggested by prior experience and the thermal analysis program. These conditions must be tested to prove the feasibility for the web-dendritic ribbon growth process of being capable of producing solar cell quality silicon in the quantities and quality needed to meet the goals of the Low Cost Silicon Solar Array Project.

Equally important to the program are the characterization facilities which have all been made operational and proven satisfactory for determination of the quality of the ribbon grown in the web-dendritic ribbon puller.

Tentative Conclusions and Recommendations

The program is too immature at this time to warrant the formation of any conclusions that would have any bearing on the goals of the program. It is expected that these will be forthcoming in the next report period.

Engineering Drawings and Sketches

The following two drawings are included in this report:

1. MOS Minority Carrier Lifetime Facility;
2. Solar Cell I-V Test Circuit.

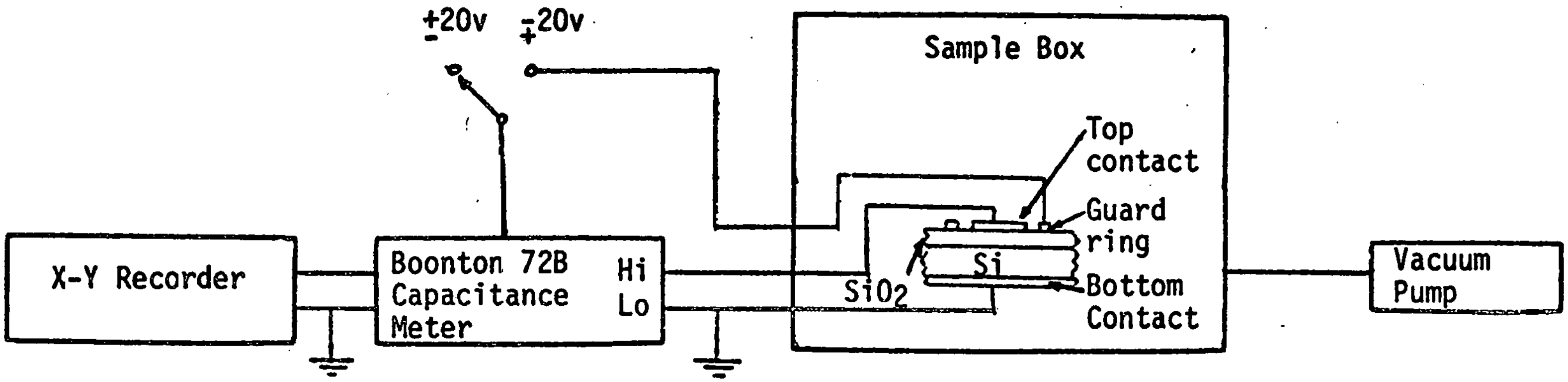

MOS Capacitance Lifetime Measuring Apparatus

Sample Box: Approximately (2 feet)^3 constructed of 3/4 inch plywood lined with 1/32 inch aluminum so as to be light and electrically tight. The box is cut on a side diagonal and hinged on the upper rear edge so as to open in a clam-shell fashion. It contains a binocular microscope, a probe positioner ring, and two vacuum sample stages.

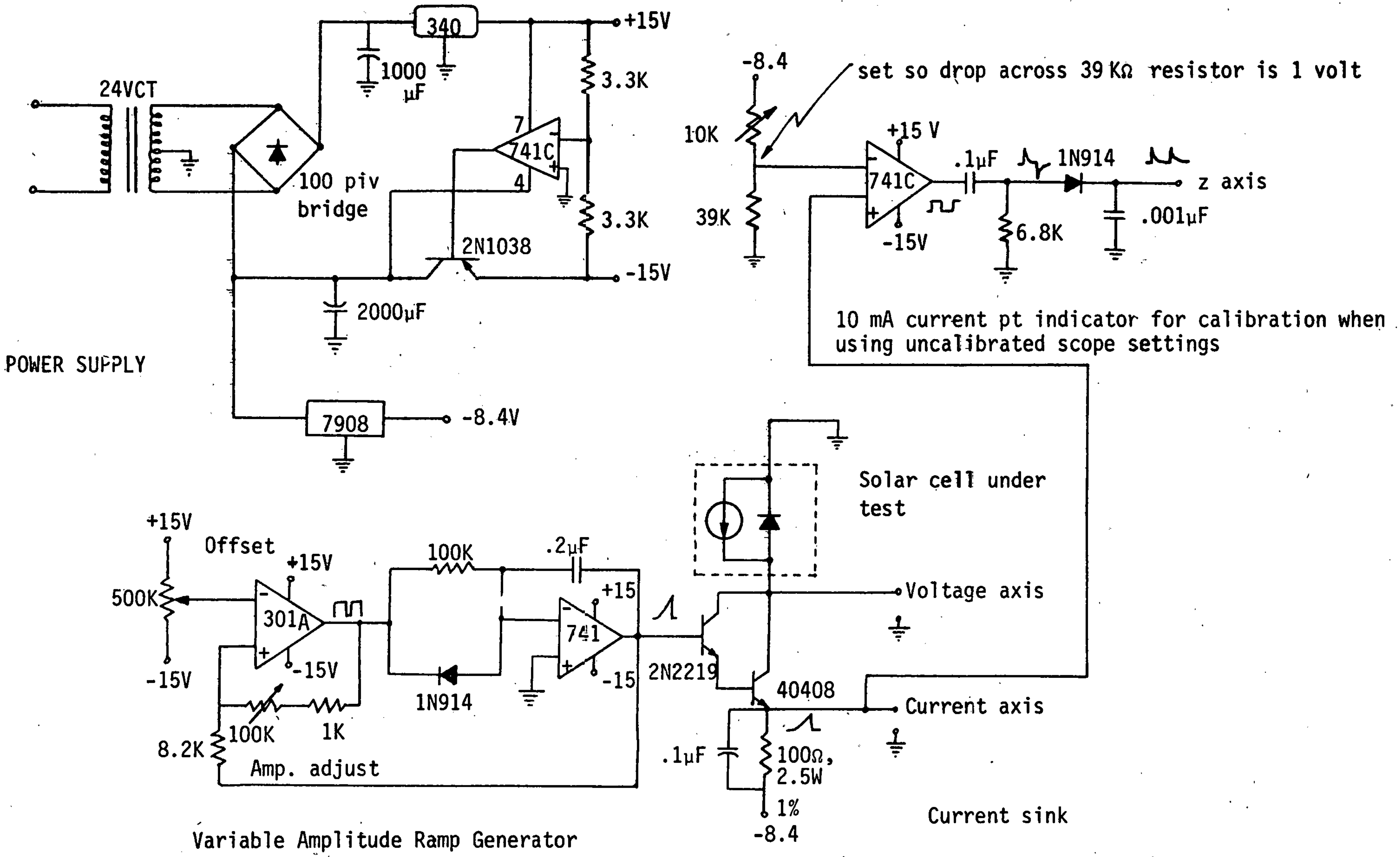

Solar Cell I - V Tester

Capable of sweeping currents from 1 to 200 mA.

Projection of Activities for Succeeding Three Months

The projected activities for the next three months are depicted in the Program Plan for this period. In summary this will consist of:

(a) growth of web-dendritic ribbon;
(b) continued thermal analysis of growth conditions;
(c) characterization of ribbon.

In addition, as a result of a Technical Direction Memorandum, dated 3/18/76, experimentation will be pursued to determine the thermal gradients in the molten Si charge.

Summary of Characterization Data

All of the structural data taken during the month was twin spacing. The data summarized here was obtained using the SEM. The studies showed for approximately a dozen different dendrites and webs that instead of three twin planes we had 5. The spacing of the lamellae between the twin planes is 0.5, 0.2, 0.2 and 3 microns on the average. Two samples did not show the 3 micron lamella; this, however, is presumably due to operator learning and poor fracturing. Two samples from a piece of web that was grown at Westinghouse prior to 1967 were examined by this technique. The results were the same which is not too surprising since a piece of this material was used as the initial seed on this contract.

Four-probe resistivity and conductivity type measurements were performed on 18 samples from 8 different web-dendritic ribbon growth runs. In all cases the conductivity was p-type and the average resistivity was 194 ohm-cms, with the lower and upper limits being 10.8 and 477 ohm-cms respectively.

TABLE 1

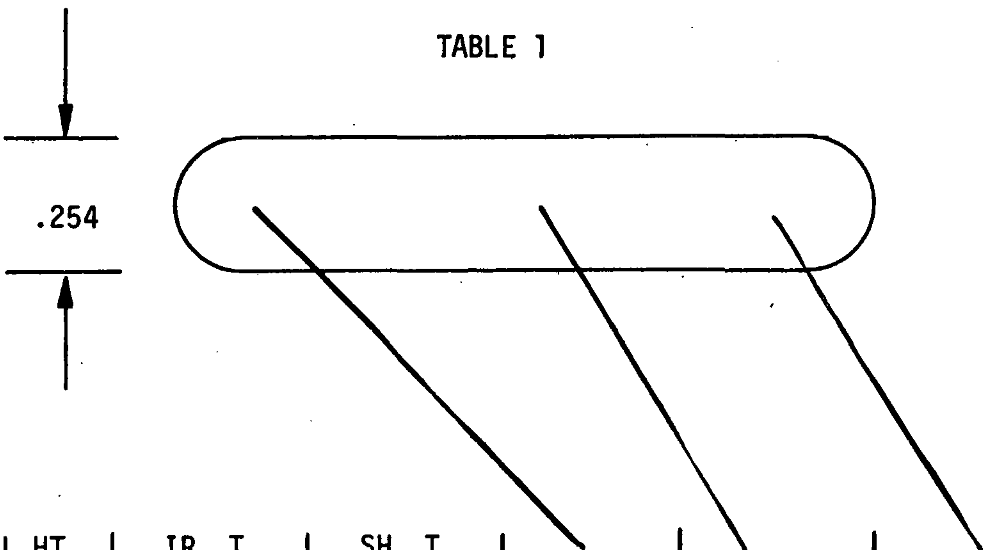

COIL HT.	IR. T. (°C)	SH. T. (°C)	(°C)	(°C)	(°C)
6 cm	1298	1276	1443	1376	1415
5.5	1309	1268	1443	1385	1421
5.0	1304	1282	1444	1376	1419
4.5	1319	1268	1438	1376	1421
4.0	1320	1255	1438	1365	1382
3.5	1315	1244	1426	1362	1399
3.0	1310	1237	1424	1360	1393

TABLE 2

T_i = temperature of the liquid-solid interface = ________________

T_s = temperature of the shield = ________________________

d_s = thickness of the shield = __________________________

d_e = thickness of the envelope = _________________________

ε_e = emissivity of the material the envelope is made of = ______________

d_1 = distance between the liquid-solid interface to the shield = ___________

d_2 = distance between the liquid-solid interface to the melt surface = ________

d_3 = distance between centerline of melt and edge of crucible = ____________

d_c = thickness of crucible wall at melt surface = ____________________

T_∞ = temperature of melt at the surface = ___________________

ε_s = emissivity of shield material = __________________

Material shield is made of = ______________________

Material envelope is made of = ____________________

Material crucible is made of = ____________________

ε_c = emissivity of crucible material = __________________

T_e = temperature of the envelope = ______________________

T_a = temperature of the surrounding atmosphere = ______________________

P_a = pressure of the surrounding atmosphere = _______________________

d_4 = diameter of envelope = ____________________

d_5 = distance between the shield (where the web is pulled) = ________________

d_w = actual web thickness = _____________________

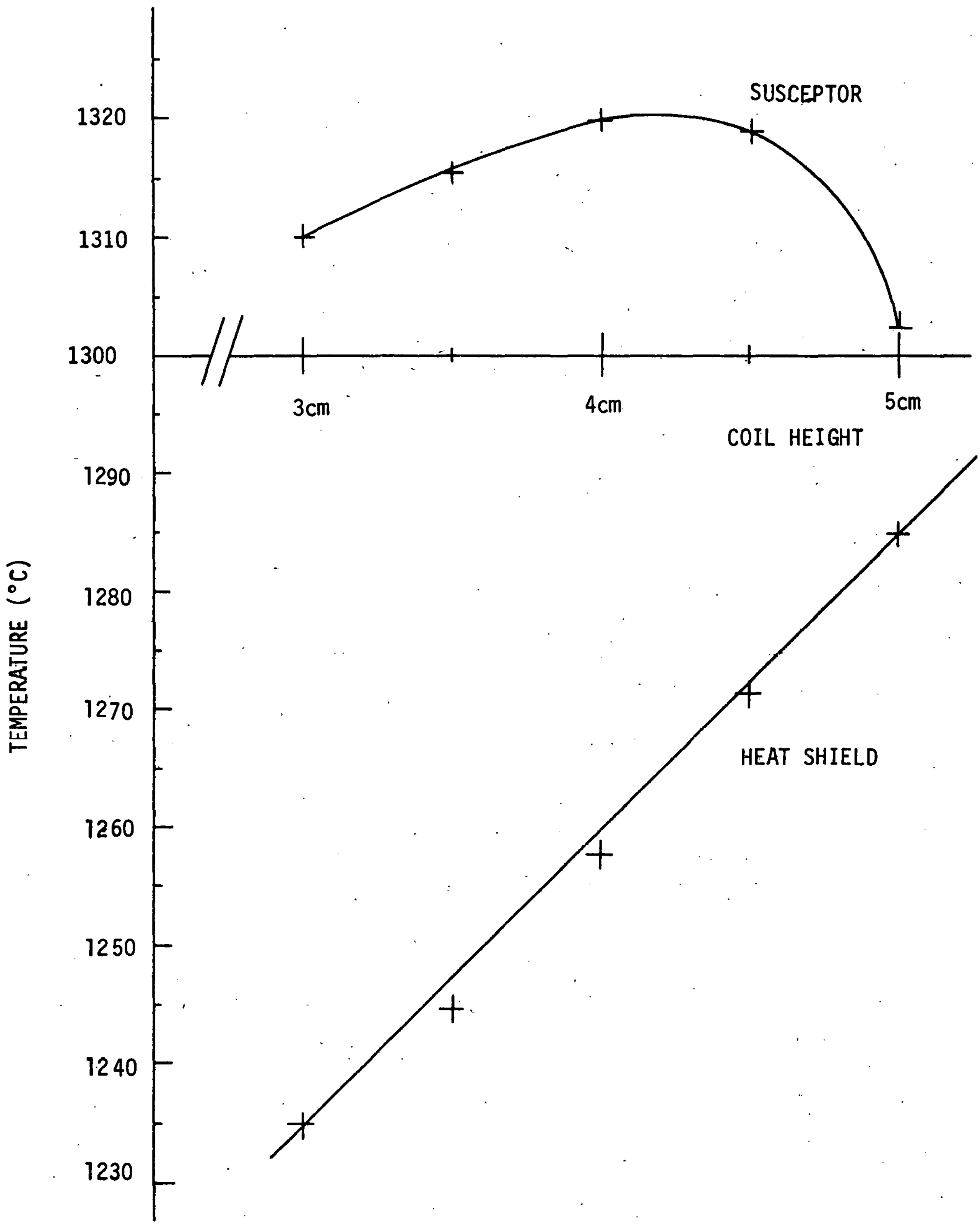
SUSCEPTOR
1320
1310
1300
3cm
4cm
5cm
COIL HEIGHT
1290
1280
1270
1260
1250
1240
1230
TEMPERATURE (°C)
HEAT SHIELD

FIGURE 1

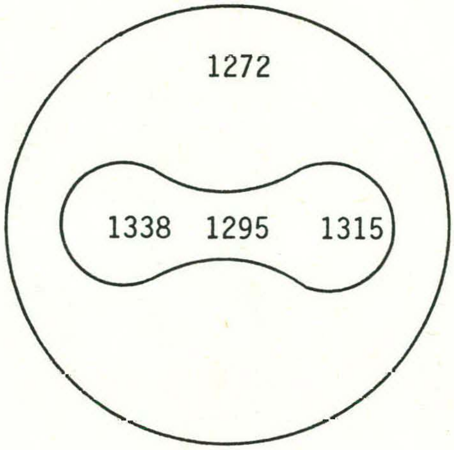

FIGURE 2.

FIGURE 3.

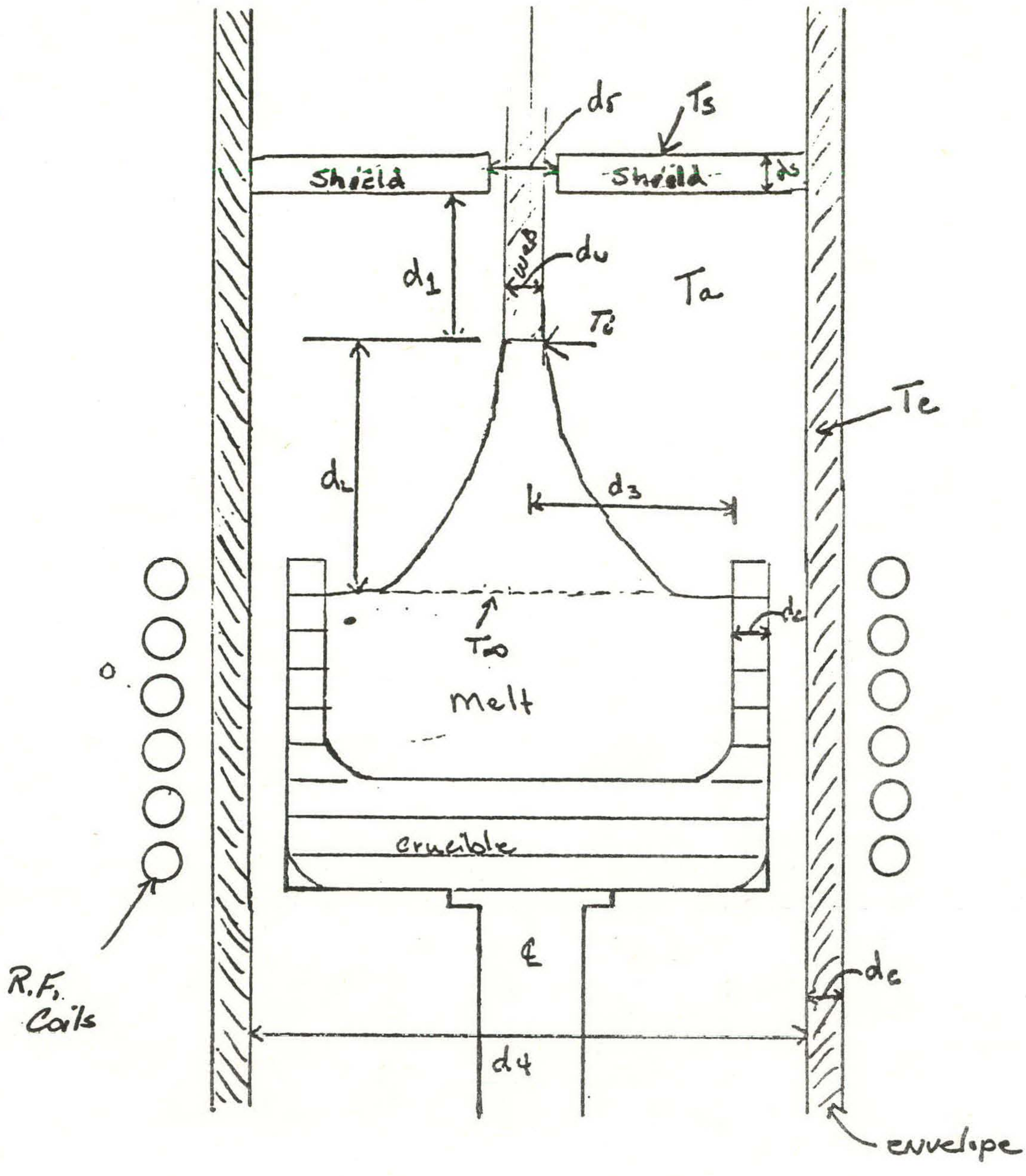

FIGURE 4 - SKETCH OF FURNACE WITH UNKNOWNS LABELED.

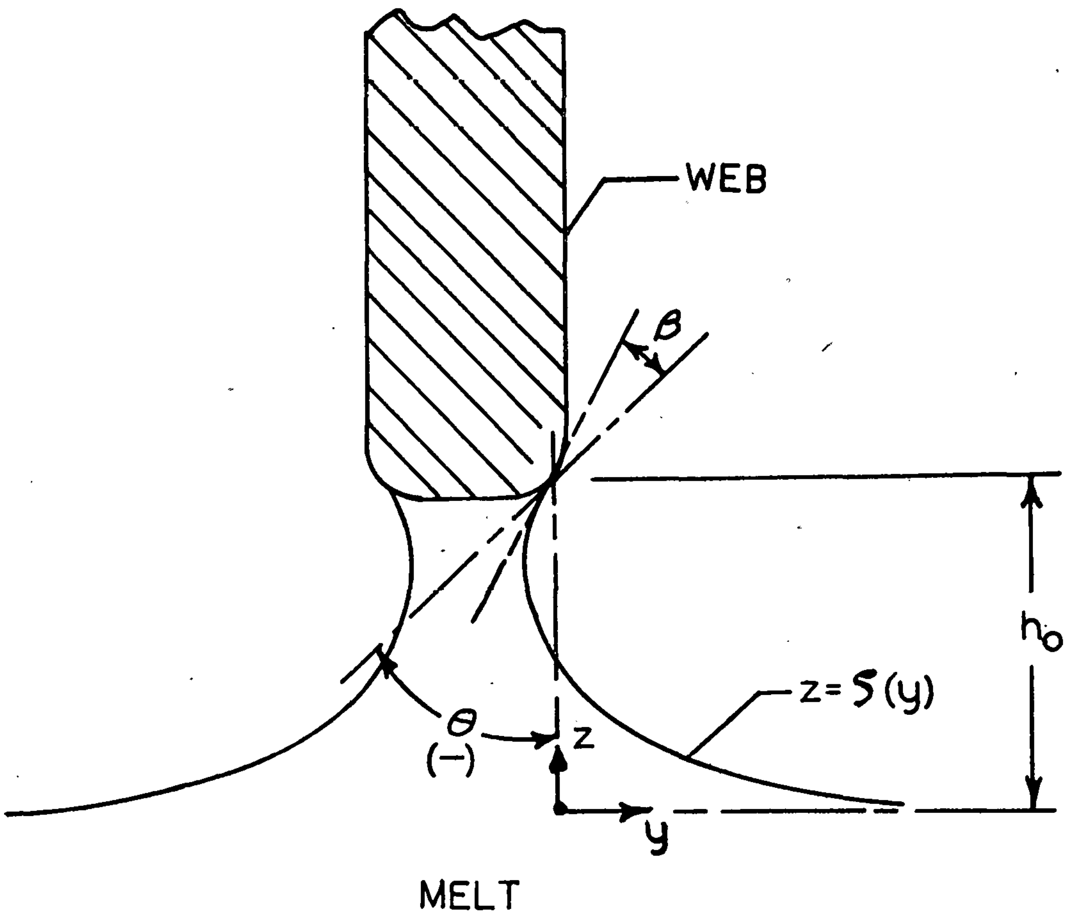

FIGURE 5. Cross-section of Web and Meniscus. β is contact or wetting angle, θ is joining angle, h_0 is height of meniscus at contact, and y and z are horizontal and vertical coordinates.

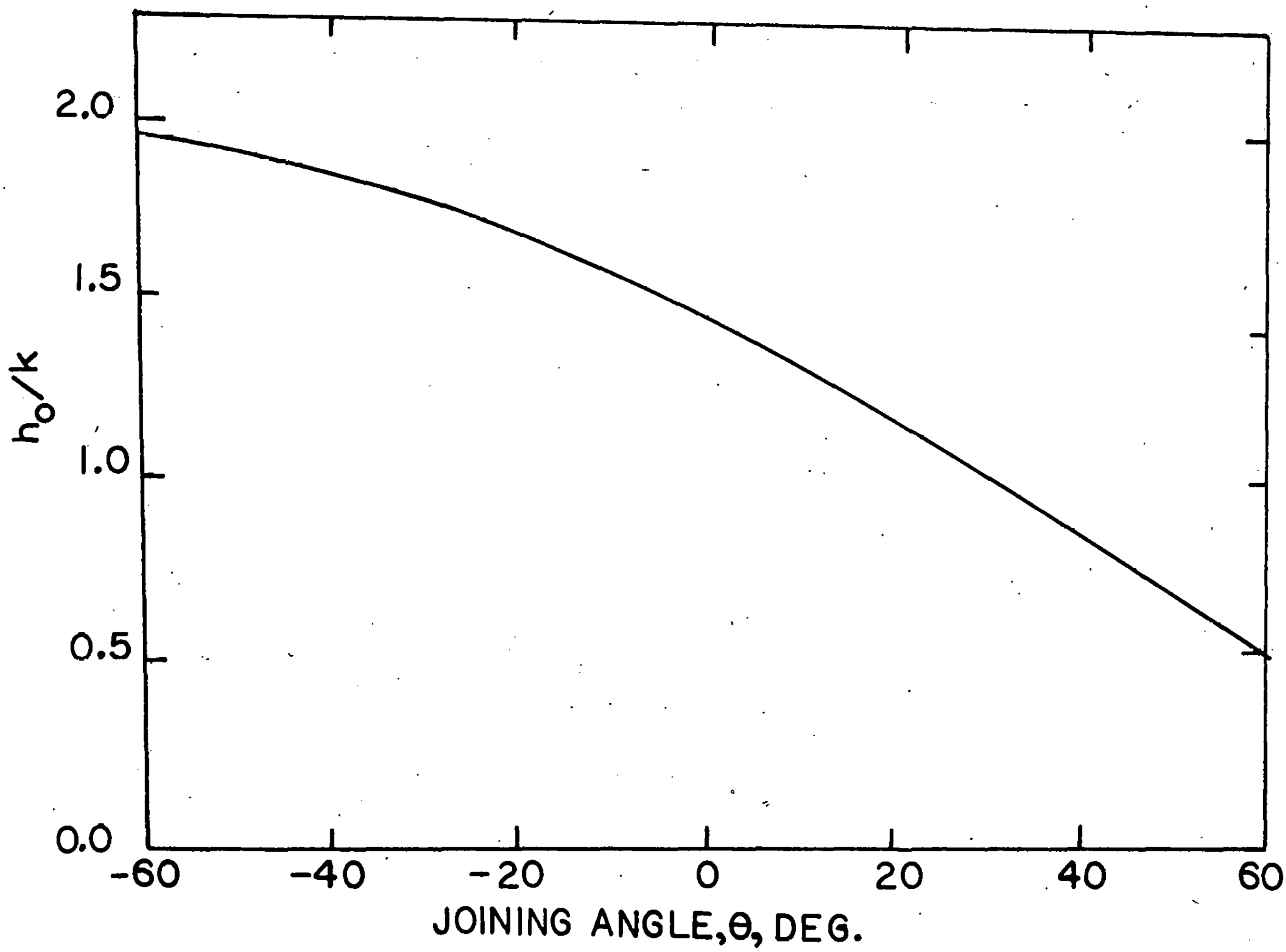

FIGURE 6. Meniscus Dimensionless Height as a Function of Joining Angle θ.

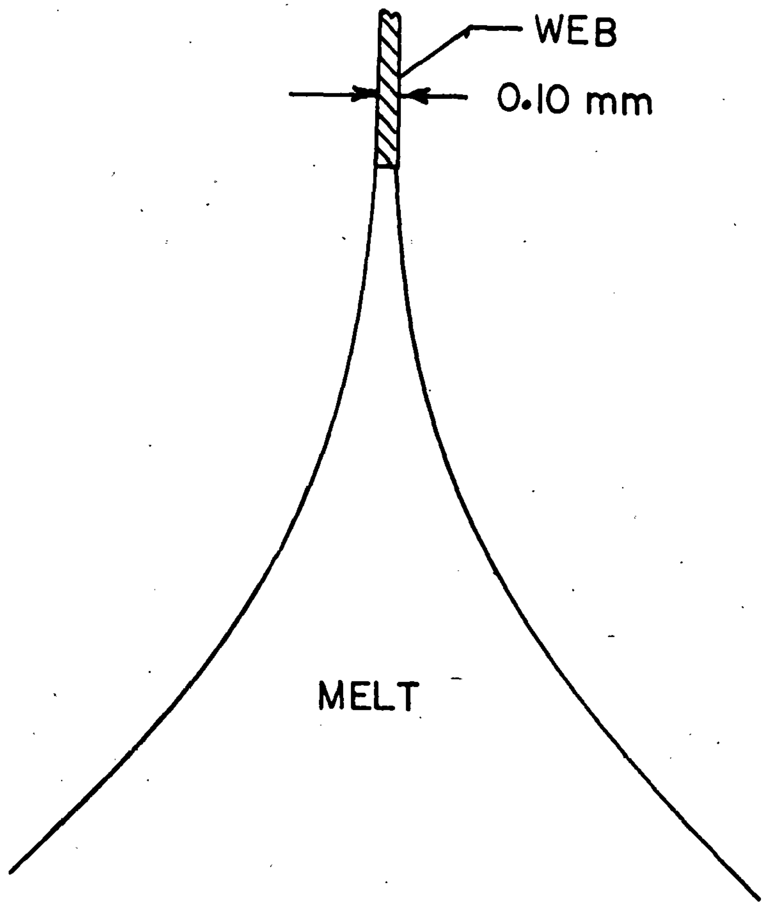

FIGURE 7. Web and Meniscus Cross-section, 0.1 mm Web Thickness and $\theta = 0^{0}$.

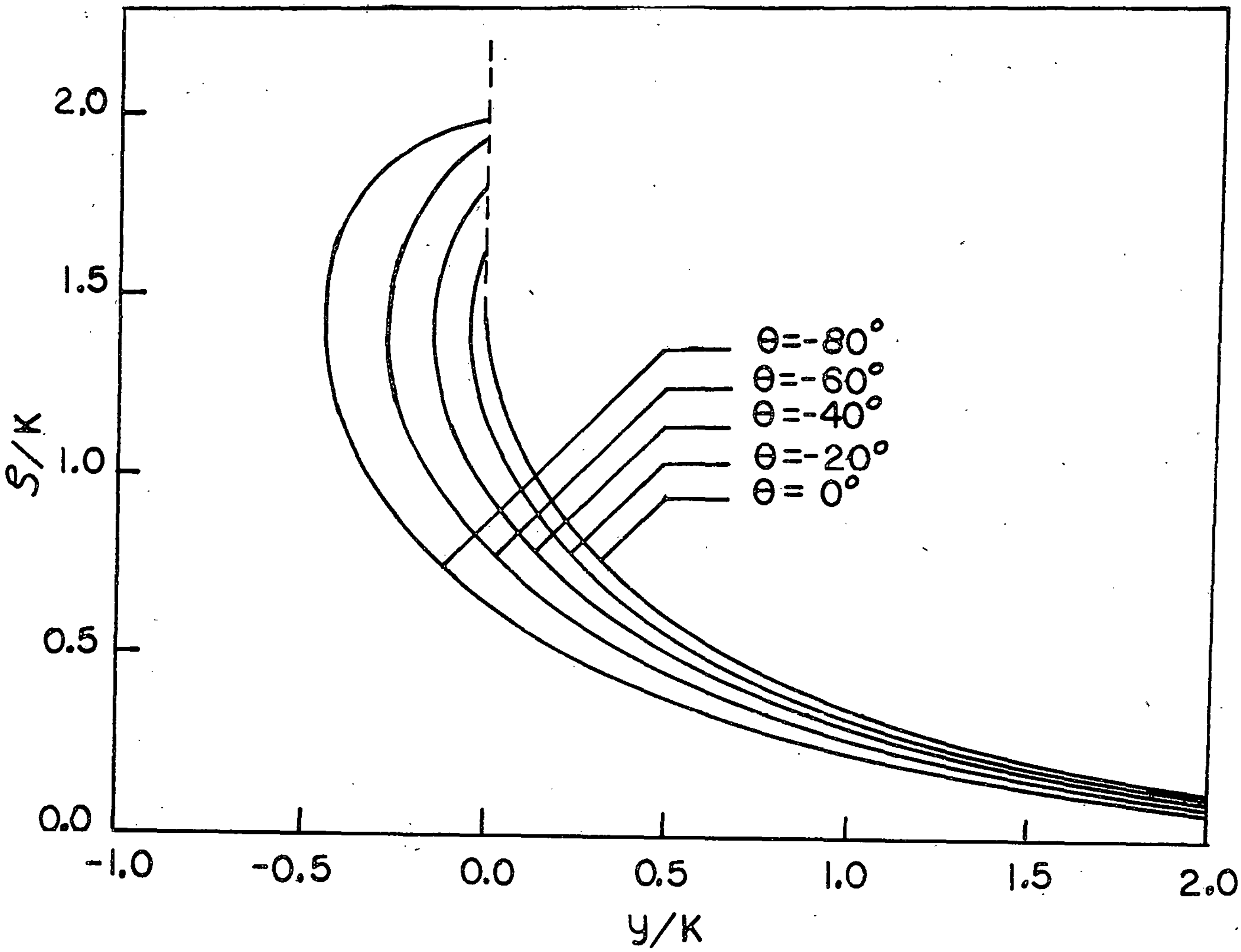

FIGURE 8. Menisci Geometry for Negative Joining Angle θ. ς/K is plotted as a function of y/K.

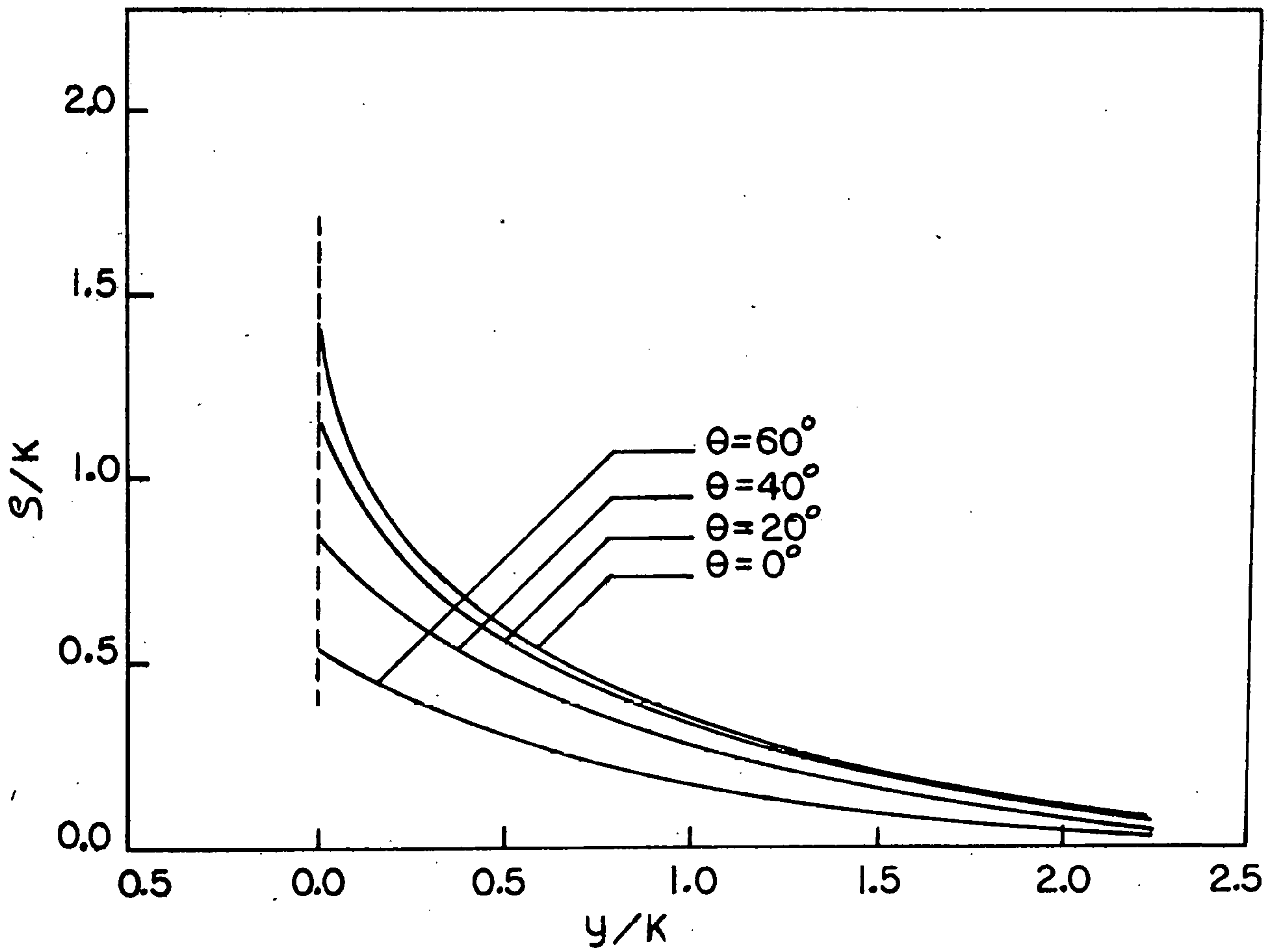

FIGURE 9. Menisci Geometry for Positive Joining Angle θ. ζ/K is plotted as a function of y/K.

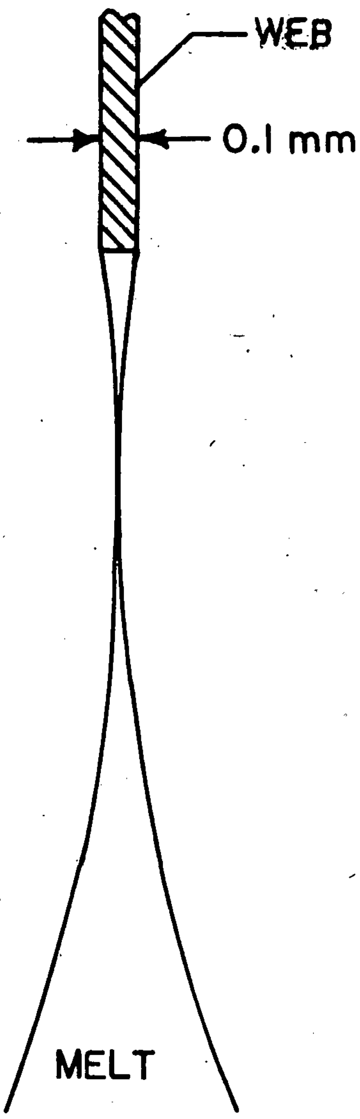

FIGURE 10. Web and Meniscus Cross-section for $\theta = -10^{\circ}$ and Silicon Melt.

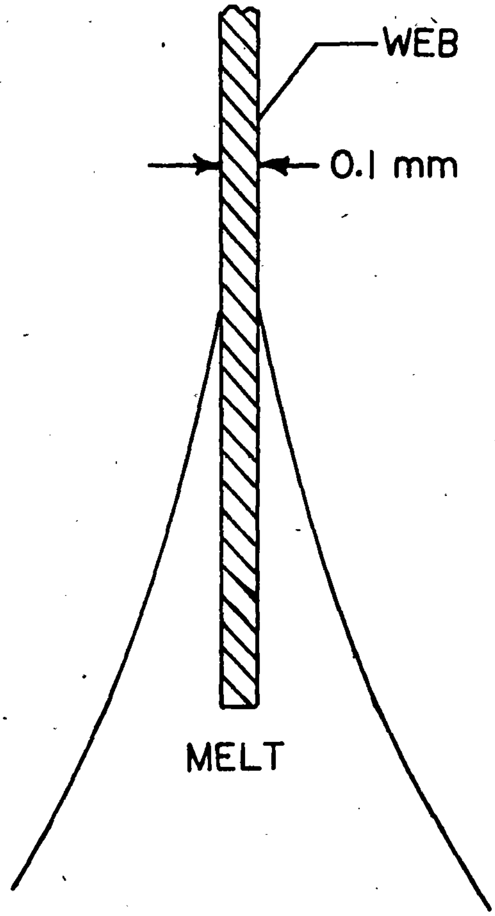

FIGURE 11. Web and Meniscus Cross-section for $\theta = 11^{o}$ and Silicon Melt.

PROGRAM PLAN

WEB-DENDRITIC RIBBON GROWTH

UNIVERSITY OF SOUTH CAROLINA

LEGEND:
H - HILBORN
F - FAUST
R - RHODES
A - RESEARCH ASSOCIATE
G - GRADUATE ASSISTANT
S - SECRETARY

PERIOD: 1 OCTOBER 1975 - 1 MAY 1977
UPDATED 17 MARCH 1976

(Figures in columns represent man hours committed)

1. Web Growth, Growth Analysis

1.1 Set up web furnace

1.1.1 Level, align, calibrate gas flow, measure physical/mechanical parameters

1.1.2 Instrument melt temperature sensors, run furnace and RF generator

1.1.3 Calibrate RF generator controls to melt temperature, no web pulling

1.2 Web growth, manual batch

1.2.1 Pull nominal web based on 1965 experience, establish measurements baseline. (Instrument melt level measurement), correlate with crystallization kinetics and seeding requirements

1.2.2 Vary pull rate, measure effects, correlate with crystallization kinetics and seeding requirements

1.2.3 Vary RF heat transfer rate, measure effects, correlate with crystallization kinetics and seeding requirements

1.2.4 Couple RF heat transfer rate and pull rate variations, measure effects, correlate with crystallization kinetics and seeding requirements

1.2.5 Final experimental design

1.2.6 Final manual variation of manipulated variables, correlation with crystallization kinetics and seeding requirements

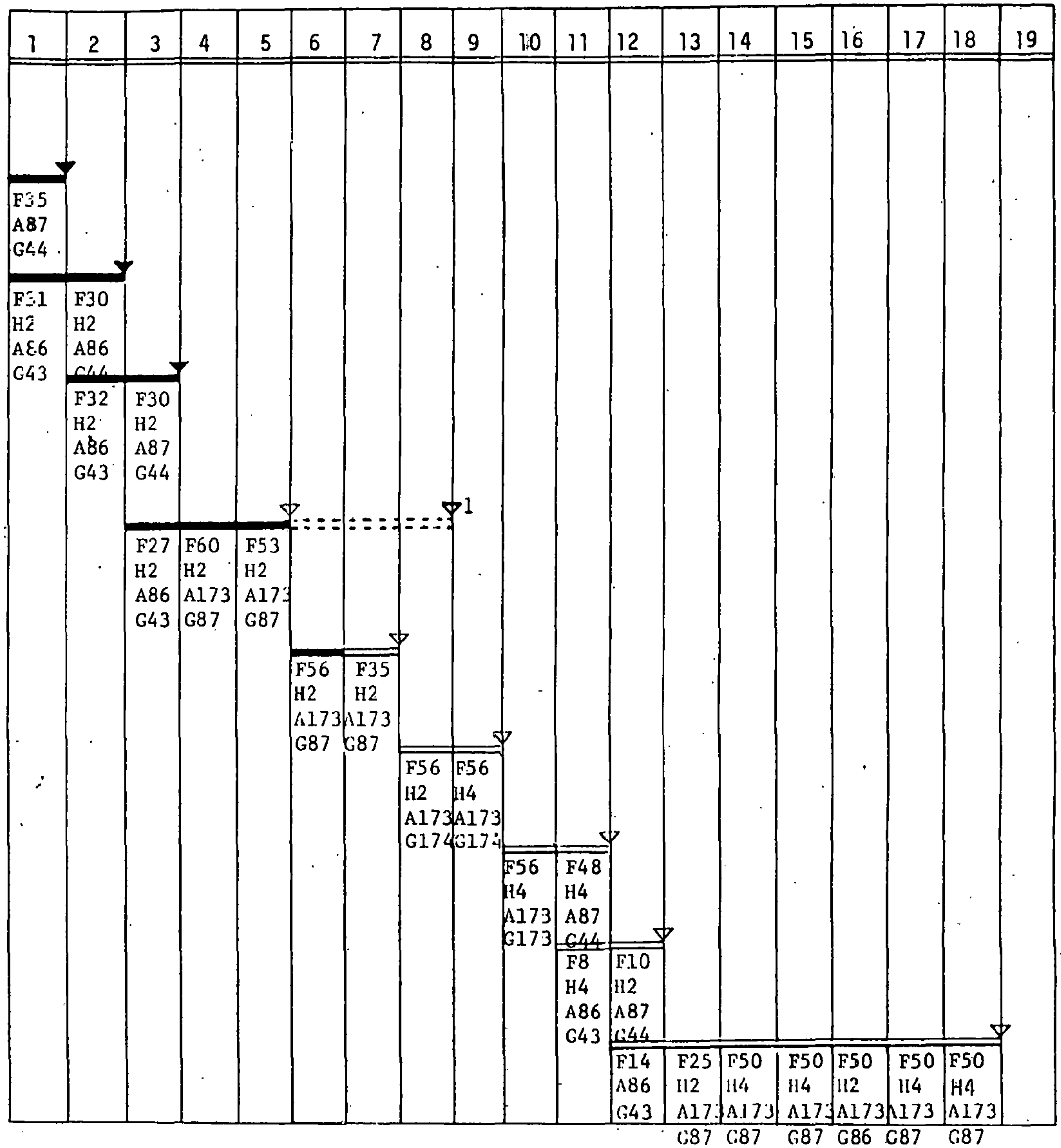

Task	1	2	3	4	5	6	7	8	9	10	11	12	13	14	15	16	17	18	19
1.3 Web growth analysis													Choice of Emphasis 1.3.1 or 1.3.2						
1.3.1 Develop semi-empirical multivariate static model from web growth manual experiments	F4 H4 R33	F4 H2 R32	F4 R20	F4 R20	F4 R16	F4 R16	F2 R16	F4 R20	F16 H4 R20	F16 H4 R20	F16 H4 R20	F2 R15	F4 R31 G87	F4 R30 G87	F4 R31 G86	F4 R30 G87	F4 R31 G86	F4 R30 G86	
1.3.2 Thermal web growth analysis			H2 R13	H2 R20 G87	R17 G87	R16 G86	R17 G87	R16 G87	F4 H4 R48 G86	F4 H4 R47 G87	F4 H4 R48 G87	R15 G86							
1.3.3 Correlate analysis, experimental data, and semi-empirical model					F4 H2 R8	F4 H2 R8	F2 H2 R8	F4 H2 R8	F40 H8 R17	F40 H8 R17	F40 H8 R17	F2 R8	F2 H2 R8	F10 H2 R8	F7 H2 R8	F10 H2 R8	F7 H2 R8	F10 H2 R8	
2. Web Characterization																			
2.1 Development of sampling strategy, prototype technique	H17 F8	H16 F8																	
2.2 Structural characterization	F3 G173	F10 G173	F20 G174	F20 G173	F20 G173	F20 G174	F12 G173	F20 G173	F51 G174	F54 G173	F51 G173	F20 G174	F20 G173	F20 G173	F20 G174	F20 G173	F20 G174	F20 G174	
2.3 Electrical characterization, web bulk silicon	H3 G130	H13 G130	H16 G130	H18 G130	H21 G130	H20 G130	H29 G130	H24 G130	H52 G130	H51 G130	H52 G130	H4 G130	H29 G130	H23 G130	H16 G130	H18 G130	H17 G130	H14 G130	
2.4 Electrical characterization, web solar cells	H3 G130	H13 G130	H15 G130	H18 G130	H20 G130	H18 G130	H28 G130	H22 G130	H51 G130	H51 G130	H51 G130	H4 G130	H28 G130	H21 G130	H15 G130	H18 G130	H18 G130	H14 G130	
3. Documentation, Program Review																			
3.1 Documentation																			
3.1.1 Initial financial management report and program plan	H26																		
3.1.2 NASA Form 533M MAR 73, JPL 3645, JPL 3645-1	H2	H2	H2	H2	H2	H2	H2	H2	H2	H2	H2	H2	H2	H2	H2	H2	H2	H2	H2

	1	2	3	4	5	6	7	8	9	10	11	12	13	14	15	16	17	18	19
3.1.3 Monthly technical progress report		H10	H8		H8	H8		H8	H8		H8	H8		H8	H8		H8	H8	
3.1.4 Quarterly report		H8	H16		H8	H16		H8	H16					H8	H16				
3.1.5 Interim summary																			
3.1.6 Annual report											H12	H24							
3.1.7 Draft final report																	H12	H24	
3.1.8 Approved final report																			H69 F87 R42
3.2 Program review, work sessions																			
3.2.1 USC in-house review		H3 F3 R3		H3 F3 R3		H3 F3 R3		H3 F3 R3		H3 F3 R3		H3 F3 R3		H3 F3 R3		H3 F3 R3		H3 F3 R3	
3.2.2 JPL program review	H8 F6 R2		H8 F6 R2		H8 F6 R2		H8 F6 R2		H8 F6 R2		H8 F6 R2		H8 F6 R2		H8 F6 R2		H8 F6 R2		
3.2.3 Task integration sessions				H30			F30			H30			F30			H30			
3.2.4 Annual workshop												H36 F36							

	1	2	3	4	5	6	7	8	9	10	11	12	13	14	15	16	17	18
3.2.5 Design and performance review				▽		▼1												
4. General Administration	H22 S87	H16 S87	H16 S87	H12 S87	H16 S87	H16 S87	H16 S87	H16 S87	H16 S87	H16 S87	H16 S87	H4 S87	H16 S87	H16 S87	H16 S87	H12 S87	H16 S87	H16 S87
5. Planned Cost (Thousands of dollars)	12.5	16.8	14.2	14.3	12.7	13.0	13.3	12.6	17.8	19.1	17.2	15.5	13.5	12.8	13.6	13.4	12.8	13.2
Incurred Cost (Thousands of dollars)																		